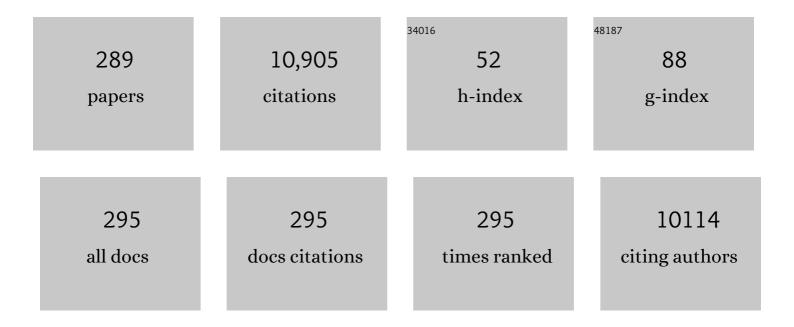
Chang-Guo Zhan

List of Publications by Year in descending order

Source: https://exaly.com/author-pdf/4372624/publications.pdf Version: 2024-02-01



#	Article	lF	CITATIONS
1	Ionization Potential, Electron Affinity, Electronegativity, Hardness, and Electron Excitation Energy: Molecular Properties from Density Functional Theory Orbital Energies. Journal of Physical Chemistry A, 2003, 107, 4184-4195.	1.1	1,134
2	A novel Hsp90 inhibitor to disrupt Hsp90/Cdc37 complex against pancreatic cancer cells. Molecular Cancer Therapeutics, 2008, 7, 162-170.	1.9	338
3	The Tumor Inhibitor and Antiangiogenic Agent Withaferin A Targets the Intermediate Filament Protein Vimentin. Chemistry and Biology, 2007, 14, 623-634.	6.2	283
4	Absolute Hydration Free Energy of the Proton from First-Principles Electronic Structure Calculations. Journal of Physical Chemistry A, 2001, 105, 11534-11540.	1.1	277
5	Identify potent SARS-CoV-2 main protease inhibitors via accelerated free energy perturbation-based virtual screening of existing drugs. Proceedings of the National Academy of Sciences of the United States of America, 2020, 117, 27381-27387.	3.3	174
6	Computational redesign of human butyrylcholinesterase for anticocaine medication. Proceedings of the United States of America, 2005, 102, 16656-16661.	3.3	171
7	Hydration of the Fluoride Anion:Â Structures and Absolute Hydration Free Energy from First-Principles Electronic Structure Calculations. Journal of Physical Chemistry A, 2004, 108, 2020-2029.	1.1	166
8	Most Efficient Cocaine Hydrolase Designed by Virtual Screening of Transition States. Journal of the American Chemical Society, 2008, 130, 12148-12155.	6.6	164
9	Electron Affinities of AlnClusters and Multiple-Fold Aromaticity of the Square Al42-Structure. Journal of the American Chemical Society, 2002, 124, 14795-14803.	6.6	162
10	Volume polarization in reaction field theory. Journal of Chemical Physics, 1998, 108, 177-192.	1.2	132
11	Fundamental Reaction Mechanism for Cocaine Hydrolysis in Human Butyrylcholinesterase. Journal of the American Chemical Society, 2003, 125, 2462-2474.	6.6	131
12	Subnanomolar Inhibitor of Cytochrome <i>bc</i> ₁ Complex Designed by Optimizing Interaction with Conformationally Flexible Residues. Journal of the American Chemical Society, 2010, 132, 185-194.	6.6	110
13	Catalytic Mechanism of Cytochrome P450 for 5′-Hydroxylation of Nicotine: Fundamental Reaction Pathways and Stereoselectivity. Journal of the American Chemical Society, 2011, 133, 7416-7427.	6.6	110
14	Reaction Pathways and Energy Barriers for Alkaline Hydrolysis of Carboxylic Acid Esters in Water Studied by a Hybrid Supermolecule-Polarizable Continuum Approach. Journal of the American Chemical Society, 2000, 122, 2621-2627.	6.6	107
15	The Nature and Absolute Hydration Free Energy of the Solvated Electron in Water. Journal of Physical Chemistry B, 2003, 107, 4403-4417.	1.2	107
16	Cavity size in reaction field theory. Journal of Chemical Physics, 1998, 109, 10543-10558.	1.2	105
17	First-Principles Determination of the Absolute Hydration Free Energy of the Hydroxide Ionâ€. Journal of Physical Chemistry A, 2002, 106, 9737-9744.	1.1	105
18	Fundamental Reaction Pathway and Free Energy Profile for Inhibition of Proteasome by Epoxomicin. Journal of the American Chemical Society, 2012, 134, 10436-10450.	6.6	100

#	Article	IF	CITATIONS
19	Modeling the Catalysis of Anti-Cocaine Catalytic Antibody: Competing Reaction Pathways and Free Energy Barriers. Journal of the American Chemical Society, 2008, 130, 5140-5149.	6.6	97
20	Reaction field effects on nitrogen shielding. Journal of Chemical Physics, 1999, 110, 1611-1622.	1.2	86
21	Determination of Two Structural Forms of Catalytic Bridging Ligand in Zincâ^'Phosphotriesterase by Molecular Dynamics Simulation and Quantum Chemical Calculation. Journal of the American Chemical Society, 1999, 121, 7279-7282.	6.6	83
22	Ligand-Based Virtual Screening Approach Using a New Scoring Function. Journal of Chemical Information and Modeling, 2012, 52, 963-974.	2.5	83
23	Decomposition Pathways of Peroxynitrous Acid:  Gas-Phase and Solution Energetics. Journal of Physical Chemistry A, 2002, 106, 3191-3196.	1.1	81
24	Thermostable Variants of Cocaine Esterase for Long-Time Protection against Cocaine Toxicity. Molecular Pharmacology, 2009, 75, 318-323.	1.0	81
25	Design, Preparation, and Characterization of High-Activity Mutants of Human Butyrylcholinesterase Specific for Detoxification of Cocaine. Molecular Pharmacology, 2011, 79, 290-297.	1.0	81
26	How Dopamine Transporter Interacts with Dopamine: Insights from Molecular Modeling and Simulation. Biophysical Journal, 2007, 93, 3627-3639.	0.2	79
27	Combined 3D-QSAR Modeling and Molecular Docking Study on Indolinone Derivatives as Inhibitors of 3-Phosphoinositide-Dependent Protein Kinase-1. Journal of Chemical Information and Modeling, 2008, 48, 1760-1772.	2.5	76
28	Free Energy Perturbation (FEP) Simulation on the Transition States of Cocaine Hydrolysis Catalyzed by Human Butyrylcholinesterase and Its Mutants. Journal of the American Chemical Society, 2007, 129, 13537-13543.	6.6	74
29	Mobility of the Active Site Bound Paraoxon and Sarin in Zinc-Phosphotriesterase by Molecular Dynamics Simulation and Quantum Chemical Calculation. Journal of the American Chemical Society, 2001, 123, 817-826.	6.6	72
30	Molecular Dynamics Simulation of Cocaine Binding with Human Butyrylcholinesterase and Its Mutants. Journal of Physical Chemistry B, 2005, 109, 4776-4782.	1.2	72
31	Mechanism for Cocaine Blocking the Transport of Dopamine: Insights from Molecular Modeling and Dynamics Simulations. Journal of Physical Chemistry B, 2009, 113, 15057-15066.	1.2	72
32	First-Principles Calculation of p <i>K</i> _a for Cocaine, Nicotine, Neurotransmitters, and Anilines in Aqueous Solution. Journal of Physical Chemistry B, 2007, 111, 10599-10605.	1.2	71
33	Catalytic Mechanisms for Cofactor-Free Oxidase-Catalyzed Reactions: Reaction Pathways of Uricase-Catalyzed Oxidation and Hydration of Uric Acid. ACS Catalysis, 2017, 7, 4623-4636.	5.5	71
34	Energy Barriers for Alkaline Hydrolysis of Carboxylic Acid Esters in Aqueous Solution by Reaction Field Calculations. Journal of Physical Chemistry A, 2000, 104, 7672-7678.	1.1	70
35	First Computational Evidence for a Catalytic Bridging Hydroxide Ion in a Phosphodiesterase Active Site. Journal of the American Chemical Society, 2001, 123, 2835-2838.	6.6	69
36	Computational Design of a Human Butyrylcholinesterase Mutant for Accelerating Cocaine Hydrolysis Based on the Transition-State Simulation. Angewandte Chemie - International Edition, 2006, 45, 653-657.	7.2	69

#	Article	IF	CITATIONS
37	Molecular insights into the mechanism of 4â€hydroxyphenylpyruvate dioxygenase inhibition: enzyme kinetics, Xâ€ray crystallography and computational simulations. FEBS Journal, 2019, 286, 975-990.	2.2	68
38	A highly efficient cocaine-detoxifying enzyme obtained by computational design. Nature Communications, 2014, 5, 3457.	5.8	67
39	Catalytic Mechanism and Energy Barriers for Butyrylcholinesterase-Catalyzed Hydrolysis of Cocaine. Biophysical Journal, 2005, 89, 3863-3872.	0.2	65
40	Characterization of a high-activity mutant of human butyrylcholinesterase against (â^')-cocaine. Chemico-Biological Interactions, 2010, 187, 148-152.	1.7	62
41	Crystal Structure of 4-Hydroxyphenylpyruvate Dioxygenase in Complex with Substrate Reveals a New Starting Point for Herbicide Discovery. Research, 2019, 2019, 2602414.	2.8	62
42	How Can (â^')-Epigallocatechin Gallate from Green Tea Prevent HIV-1 Infection? Mechanistic Insights from Computational Modeling and the Implication for Rational Design of Anti-HIV-1 Entry Inhibitors. Journal of Physical Chemistry B, 2006, 110, 2910-2917.	1.2	61
43	Structure-based methods for predicting target mutation-induced drug resistance and rational drug design to overcome the problem. Drug Discovery Today, 2012, 17, 1121-1126.	3.2	60
44	Uricases as Therapeutic Agents to Treat Refractory Gout: Current States and Future Directions. Drug Development Research, 2012, 73, 66-72.	1.4	59
45	Reaction Pathway and Free Energy Profile for Papain-Catalyzed Hydrolysis of <i>N</i> -Acetyl-Phe-Gly 4-Nitroanilide. Biochemistry, 2013, 52, 5145-5154.	1.2	59
46	Theoretical Studies of Fundamental Pathways for Alkaline Hydrolysis of Carboxylic Acid Esters in Gas Phase. Journal of the American Chemical Society, 2000, 122, 1522-1530.	6.6	58
47	Free-Energy Perturbation Simulation on Transition States and Redesign of Butyrylcholinesterase. Biophysical Journal, 2009, 96, 1931-1938.	0.2	58
48	Theoretical Studies of the Transition-State Structures and Free Energy Barriers for Base-Catalyzed Hydrolysis of Amides. Journal of Physical Chemistry A, 2006, 110, 12644-12652.	1.1	56
49	Long-acting cocaine hydrolase for addiction therapy. Proceedings of the National Academy of Sciences of the United States of America, 2016, 113, 422-427.	3.3	56
50	Coordination number of zinc ions in the phosphotriesterase active site by molecular dynamics and quantum mechanics. Journal of Computational Chemistry, 2003, 24, 368-378.	1.5	54
51	Assessing the Regioselectivity of OleD-Catalyzed Glycosylation with a Diverse Set of Acceptors. Journal of Natural Products, 2013, 76, 279-286.	1.5	54
52	Arylquins target vimentin to trigger Par-4 secretion for tumor cell apoptosis. Nature Chemical Biology, 2014, 10, 924-926.	3.9	54
53	QSAR modeling of mono- and bis-quaternary ammonium salts that act as antagonists at neuronal nicotinic acetylcholine receptors mediating dopamine release. Bioorganic and Medicinal Chemistry, 2006, 14, 3017-3037.	1.4	53
54	Reaction Pathway and Free-Energy Barrier for Reactivation of Dimethylphosphoryl-Inhibited Human Acetylcholinesterase. Journal of Physical Chemistry B, 2009, 113, 16226-16236.	1.2	53

#	Article	IF	CITATIONS
55	Fundamental Reaction Mechanism and Free Energy Profile for (â^')-Cocaine Hydrolysis Catalyzed by Cocaine Esterase. Journal of the American Chemical Society, 2009, 131, 11964-11975.	6.6	53
56	Free Energies of Solvation with Surface, Volume, and Local Electrostatic Effects and Atomic Surface Tensions to Represent the First Solvation Shell. Journal of Chemical Theory and Computation, 2010, 6, 1109-1117.	2.3	53
57	Accurate heats of formation and acidities for H3PO4, H2SO4, and H2CO3 from ab initio electronic structure calculations. International Journal of Quantum Chemistry, 2005, 102, 775-784.	1.0	52
58	Modeling Effects of Oxyanion Hole on the Ester Hydrolysis Catalyzed by Human Cholinesterases. Journal of Physical Chemistry B, 2005, 109, 23070-23076.	1.2	52
59	Active Site Gating and Substrate Specificity of Butyrylcholinesterase and Acetylcholinesterase: Insights from Molecular Dynamics Simulations. Journal of Physical Chemistry B, 2011, 115, 8797-8805.	1.2	52
60	Are pharmacokinetic approaches feasible for treatment of cocaine addiction and overdose?. Future Medicinal Chemistry, 2012, 4, 125-128.	1.1	52
61	First-principle studies of intermolecular and intramolecular catalysis of protonated cocaine. Journal of Computational Chemistry, 2005, 26, 980-986.	1.5	50
62	Modeling evolution of hydrogen bonding and stabilization of transition states in the process of cocaine hydrolysis catalyzed by human butyrylcholinesterase. Proteins: Structure, Function and Bioinformatics, 2005, 62, 99-110.	1.5	50
63	Fluorinated <i>N</i> , <i>N</i> -Dialkylaminostilbenes Repress Colon Cancer by Targeting Methionine <i>S</i> -Adenosyltransferase 2A. ACS Chemical Biology, 2013, 8, 796-803.	1.6	50
64	Improved Prediction of Blood–Brain Barrier Permeability Through Machine Learning with Combined Use of Molecular Property-Based Descriptors and Fingerprints. AAPS Journal, 2018, 20, 54.	2.2	50
65	Computational Design and Discovery of Conformationally Flexible Inhibitors of Acetohydroxyacid Synthase to Overcome Drug Resistance Associated with the W586L Mutation. ChemMedChem, 2008, 3, 1203-1206.	1.6	49
66	Understanding the Mechanism of Drug Resistance Due to a Codon Deletion in Protoporphyrinogen Oxidase through Computational Modeling. Journal of Physical Chemistry B, 2009, 113, 4865-4875.	1.2	47
67	Reaction Pathway and Free Energy Profile for Butyrylcholinesterase-Catalyzed Hydrolysis of Acetylcholine. Journal of Physical Chemistry B, 2011, 115, 1315-1322.	1.2	47
68	Novel human mPGES-1 inhibitors identified through structure-based virtual screening. Bioorganic and Medicinal Chemistry, 2011, 19, 6077-6086.	1.4	47
69	Mutation of Tyrosine 470 of Human Dopamine Transporter is Critical for HIV-1 Tat-Induced Inhibition of Dopamine Transport and Transporter Conformational Transitions. Journal of NeuroImmune Pharmacology, 2013, 8, 975-987.	2.1	47
70	Absolute Binding Free Energy Calculation and Design of a Subnanomolar Inhibitor of Phosphodiesterase-10. Journal of Medicinal Chemistry, 2019, 62, 2099-2111.	2.9	47
71	Modeling Multiple Species of Nicotine and Deschloroepibatidine Interacting with α4β2 Nicotinic Acetylcholine Receptor:Â From Microscopic Binding to Phenomenological Binding Affinity. Journal of the American Chemical Society, 2005, 127, 14401-14414.	6.6	46
72	Modeling Subtype-Selective Agonists Binding with α4β2 and α7 Nicotinic Acetylcholine Receptors: Effects of Local Binding and Long-Range Electrostatic Interactions. Journal of Medicinal Chemistry, 2006, 49, 7661-7674.	2.9	46

#	Article	IF	CITATIONS
73	Structure-and-mechanism-based design and discovery of therapeutics for cocaine overdose and addiction. Organic and Biomolecular Chemistry, 2008, 6, 836-843.	1.5	46
74	Theoretical Studies of Competing Reaction Pathways and Energy Barriers for Alkaline Ester Hydrolysis of Cocaine. Journal of Physical Chemistry A, 2001, 105, 1296-1301.	1.1	45
75	Theoretical Determination of Two Structural Forms of the Active Site in Cadmium-Containing Phosphotriesterases. Journal of Physical Chemistry B, 2002, 106, 717-722.	1.2	45
76	Structural analysis of thermostabilizing mutations of cocaine esterase. Protein Engineering, Design and Selection, 2010, 23, 537-547.	1.0	45
77	Understanding Microscopic Binding of Human Microsomal Prostaglandin E Synthase-1 (mPGES-1) Trimer with Substrate PGH ₂ and Cofactor GSH: Insights from Computational Alanine Scanning and Site-directed Mutagenesis. Journal of Physical Chemistry B, 2010, 114, 5605-5616.	1.2	45
78	Computational Mutation Scanning and Drug Resistance Mechanisms of HIV-1 Protease Inhibitors. Journal of Physical Chemistry B, 2010, 114, 9663-9676.	1.2	45
79	Proteasome Inhibitors with Pyrazole Scaffolds from Structure-Based Virtual Screening. Journal of Medicinal Chemistry, 2015, 58, 2036-2041.	2.9	45
80	Design of High-Activity Mutants of Human Butyrylcholinesterase against (â^')-Cocaine: Structural and Energetic Factors Affecting the Catalytic Efficiency. Biochemistry, 2010, 49, 9113-9119.	1.2	44
81	Modeling of Pharmacokinetics of Cocaine in Human Reveals the Feasibility for Development of Enzyme Therapies for Drugs of Abuse. PLoS Computational Biology, 2012, 8, e1002610.	1.5	43
82	Computational Simulations of the Interactions between Acetyl-Coenzyme-A Carboxylase and Clodinafop: Resistance Mechanism Due to Active and Nonactive Site Mutations. Journal of Chemical Information and Modeling, 2009, 49, 1936-1943.	2.5	42
83	Model of Human Butyrylcholinesterase Tetramer by Homology Modeling and Dynamics Simulation. Journal of Physical Chemistry B, 2009, 113, 6543-6552.	1.2	42
84	Understanding the structure–activity and structure–selectivity correlation of cyclic guanine derivatives as phosphodiesterase-5 inhibitors by molecular docking, CoMFA and CoMSIA analyses. Bioorganic and Medicinal Chemistry, 2006, 14, 1462-1473.	1.4	41
85	Cocaine Esterase Prevents Cocaine-Induced Toxicity and the Ongoing Intravenous Self-Administration of Cocaine in Rats. Journal of Pharmacology and Experimental Therapeutics, 2009, 331, 445-455.	1.3	41
86	Molecular Mechanism of HIV-1 Tat Interacting with Human Dopamine Transporter. ACS Chemical Neuroscience, 2015, 6, 658-665.	1.7	41
87	Molecular Basis of the Selectivity of the Immunoproteasome Catalytic Subunit LMP2-Specific Inhibitor Revealed by Molecular Modeling and Dynamics Simulations. Journal of Physical Chemistry B, 2010, 114, 12333-12339.	1.2	40
88	Kinetic characterization of high-activity mutants of human butyrylcholinesterase for the cocaine metabolite norcocaine. Biochemical Journal, 2014, 457, 197-206.	1.7	39
89	Theoretical Determination of Chromophores in the Chromogenic Effects of Aromatic Neurotoxicants. Journal of the American Chemical Society, 2002, 124, 2744-2752.	6.6	38
90	The gas and solution phase acidities of HNO, HOONO, HONO, and HONO2. International Journal of Mass Spectrometry, 2003, 227, 421-438.	0.7	38

6

#	Article	IF	CITATIONS
91	Theoretical Determination of Activation Free Energies for Alkaline Hydrolysis of Cyclic and Acyclic Phosphodiesters in Aqueous Solution. Journal of Physical Chemistry A, 2004, 108, 6407-6413.	1.1	38
92	Bioactive Permethrin/β-Cyclodextrin Inclusion Complex. Journal of Physical Chemistry B, 2006, 110, 7044-7048.	1.2	38
93	Rational Design, Preparation, and Characterization of a Therapeutic Enzyme Mutant with Improved Stability and Function for Cocaine Detoxification. ACS Chemical Biology, 2014, 9, 1764-1772.	1.6	37
94	Characterization of a Catalytic Ligand Bridging Metal Ions in Phosphodiesterases 4 and 5 by Molecular Dynamics Simulations and Hybrid Quantum Mechanical/Molecular Mechanical Calculations. Biophysical Journal, 2006, 91, 1858-1867.	0.2	36
95	Structural and functional characterization of human microsomal prostaglandin E synthase-1 by computational modeling and site-directed mutagenesis. Bioorganic and Medicinal Chemistry, 2006, 14, 3553-3562.	1.4	36
96	Formation and Stability of G-Quadruplexes Self-Assembled from Guanine-Rich Strands. Chemistry - A European Journal, 2007, 13, 945-949.	1.7	36
97	Fundamental Reaction Pathway for Peptide Metabolism by Proteasome: Insights from First-Principles Quantum Mechanical/Molecular Mechanical Free Energy Calculations. Journal of Physical Chemistry B, 2013, 117, 13418-13434.	1.2	36
98	Fundamental Reaction Pathway and Free Energy Profile for Butyrylcholinesterase-Catalyzed Hydrolysis of Heroin. Biochemistry, 2013, 52, 6467-6479.	1.2	35
99	Gene Transfer of Mutant Mouse Cholinesterase Provides High Lifetime Expression and Reduced Cocaine Responses with No Evident Toxicity. PLoS ONE, 2013, 8, e67446.	1.1	35
100	Fundamental Reaction Pathways and Free-Energy Barriers for Ester Hydrolysis of Intracellular Second-Messenger 3â€~,5â€~-Cyclic Nucleotide. Journal of Physical Chemistry A, 2004, 108, 3789-3797.	1.1	34
101	Reaction Pathway and Free Energy Profiles for Butyrylcholinesterase-Catalyzed Hydrolysis of Acetylthiocholine. Biochemistry, 2012, 51, 1297-1305.	1.2	34
102	Cyclic GMP–mediated memory enhancement in the object recognition test by inhibitors of phosphodiesterase-2 in mice. Psychopharmacology, 2016, 233, 447-456.	1.5	34
103	Structure-based discovery of mPGES-1 inhibitors suitable for preclinical testing in wild-type mice as a new generation of anti-inflammatory drugs. Scientific Reports, 2018, 8, 5205.	1.6	34
104	Preparation and <i>inÂvivo</i> characterization of a cocaine hydrolase engineered from human butyrylcholinesterase for metabolizing cocaine. Biochemical Journal, 2013, 453, 447-454.	1.7	33
105	A quantitative LC–MS/MS method for simultaneous determination of cocaine and its metabolites in whole blood. Journal of Pharmaceutical and Biomedical Analysis, 2017, 134, 243-251.	1.4	33
106	Talin2-mediated traction force drives matrix degradation and cell invasion. Journal of Cell Science, 2016, 129, 3661-3674.	1.2	32
107	Rational Redesign of Enzyme via the Combination of Quantum Mechanics/Molecular Mechanics, Molecular Dynamics, and Structural Biology Study. Journal of the American Chemical Society, 2021, 143, 15674-15687.	6.6	32
108	A Thermally Stable Form of Bacterial Cocaine Esterase: A Potential Therapeutic Agent for Treatment of Cocaine Abuse. Molecular Pharmacology, 2010, 77, 593-600.	1.0	31

#	Article	IF	CITATIONS
109	Substrate selectivity of high-activity mutants of human butyrylcholinesterase. Organic and Biomolecular Chemistry, 2013, 11, 7477.	1.5	31
110	Mccrearamycins A–D, Geldanamycinâ€Đerived Cyclopentenone Macrolactams from an Eastern Kentucky Abandoned Coal Mine Microbe. Angewandte Chemie - International Edition, 2017, 56, 2994-2998.	7.2	31
111	Rational design of an enzyme mutant for anti-cocaine therapeutics. Journal of Computer-Aided Molecular Design, 2008, 22, 661-671.	1.3	30
112	Recent progress in protein drug design and discovery with a focus on novel approaches to the development of anticocaine medications. Future Medicinal Chemistry, 2009, 1, 515-528.	1.1	30
113	Why Does the G117H Mutation Considerably Improve the Activity of Human Butyrylcholinesterase against Sarin? Insights from Quantum Mechanical/Molecular Mechanical Free Energy Calculations. Biochemistry, 2012, 51, 8980-8992.	1.2	30
114	Fast Prediction of Binding Affinities of the SARS-CoV-2 Spike Protein Mutant N501Y (UK Variant) with ACE2 and Miniprotein Drug Candidates. Journal of Physical Chemistry B, 2021, 125, 4330-4336.	1.2	30
115	Microscopic Modes and Free Energies of 3-Phosphoinositide-Dependent Kinase-1 (PDK1) Binding with Celecoxib and Other Inhibitors. Journal of Physical Chemistry B, 2006, 110, 26365-26374.	1.2	29
116	Modeling Binding Modes of α7 Nicotinic Acetylcholine Receptor with Ligands: The Roles of Gln117 and Other Residues of the Receptor in Agonist Binding. Journal of Medicinal Chemistry, 2008, 51, 6293-6302.	2.9	29
117	Enzyme-therapy approaches for the treatment of drug overdose and addiction. Future Medicinal Chemistry, 2011, 3, 9-13.	1.1	29
118	Kinetic characterization of human butyrylcholinesterase mutants for the hydrolysis of cocaethylene. Biochemical Journal, 2014, 460, 447-457.	1.7	29
119	Mutations at Tyrosine 88, Lysine 92 and Tyrosine 470 of Human Dopamine Transporter Result in an Attenuation of HIV-1 Tat-Induced Inhibition of Dopamine Transport. Journal of NeuroImmune Pharmacology, 2015, 10, 122-135.	2.1	29
120	Plant-expressed cocaine hydrolase variants of butyrylcholinesterase exhibit altered allosteric effects of cholinesterase activity and increased inhibitor sensitivity. Scientific Reports, 2017, 7, 10419.	1.6	29
121	Bond strength and bond angles for hybrid orbitals composed of arbitrary sets of orbital angular momentum quantum number. International Journal of Quantum Chemistry, 1987, 32, 13-18.	1.0	28
122	First-principles studies of C-13 NMR chemical shift tensors of amino acids in crystal state. Computational and Theoretical Chemistry, 2004, 682, 73-82.	1.5	28
123	Human Microsomal Prostaglandin E Synthase-1 (mPGES-1) Binding with Inhibitors and the Quantitative Structureâ´'Activity Correlation. Journal of Chemical Information and Modeling, 2008, 48, 179-185.	2.5	28
124	Reaction pathways and free energy profiles for cholinesterase-catalyzed hydrolysis of 6-monoacetylmorphine. Organic and Biomolecular Chemistry, 2014, 12, 2214-2227.	1.5	28
125	Fundamental reaction pathway and free energy profile of proteasome inhibition by syringolin A (SylA). Organic and Biomolecular Chemistry, 2015, 13, 6857-6865.	1.5	28
126	Computational neural network analysis of the affinity of lobeline and tetrabenazine analogs for the vesicular monoamine transporter-2. Bioorganic and Medicinal Chemistry, 2007, 15, 2975-2992.	1.4	27

#	Article	IF	CITATIONS
127	Modeling in vitro inhibition of butyrylcholinesterase using molecular docking, multi-linear regression and artificial neural network approaches. Bioorganic and Medicinal Chemistry, 2014, 22, 538-549.	1.4	27
128	Metabolic Enzymes of Cocaine Metabolite Benzoylecgonine. ACS Chemical Biology, 2016, 11, 2186-2194.	1.6	27
129	Role of glutamine 148 of human 15-hydroxyprostaglandin dehydrogenase in catalytic oxidation of prostaglandin E2. Bioorganic and Medicinal Chemistry, 2006, 14, 6486-6491.	1.4	26
130	Modeling Differential Binding of α4β2 Nicotinic Acetylcholine Receptor with Agonists and Antagonists. Journal of the American Chemical Society, 2008, 130, 16691-16696.	6.6	26
131	Reaction Pathway and Free Energy Profile for Cocaine Hydrolase-Catalyzed Hydrolysis of (â^')-Cocaine. Journal of Chemical Theory and Computation, 2012, 8, 1426-1435.	2.3	26
132	Crystal structure of Bacillus fastidious uricase reveals an unexpected folding of the C-terminus residues crucial for thermostability under physiological conditions. Applied Microbiology and Biotechnology, 2015, 99, 7973-7986.	1.7	26
133	Computational and Experimental Insights into the Mechanism of Substrate Recognition and Feedback Inhibition of Protoporphyrinogen Oxidase. PLoS ONE, 2013, 8, e69198.	1.1	26
134	Modeling and Re-Engineering of Azotobacter vinelandii Alginate Lyase to Enhance Its Catalytic Efficiency for Accelerating Biofilm Degradation. PLoS ONE, 2016, 11, e0156197.	1.1	26
135	Computational characterization of how the VX nerve agent binds human serum paraoxonase 1. Journal of Molecular Modeling, 2011, 17, 97-109.	0.8	25
136	Reaction Pathways and Free Energy Barriers for Alkaline Hydrolysis of Insecticide 2-Trimethylammonioethyl Methylphosphonofluoridate and Related Organophosphorus Compounds:Â Electrostatic and Steric Effects. Journal of Organic Chemistry, 2004, 69, 8451-8458.	1.7	24
137	Clinical Potential of an Enzyme-based Novel Therapy for Cocaine Overdose. Scientific Reports, 2017, 7, 15303.	1.6	24
138	Computational Determination of Binding Structures and Free Energies of Phosphodiesterase-2 with Benzo[1,4]diazepin-2-one Derivatives. Journal of Physical Chemistry B, 2010, 114, 16020-16028.	1.2	23
139	Free Energy Perturbation Simulation on Transition States and High-Activity Mutants of Human Butyrylcholinesterase for (â~')-Cocaine Hydrolysis. Journal of Physical Chemistry B, 2010, 114, 10889-10896.	1.2	23
140	Understanding Microscopic Binding of Human Microsomal Prostaglandin E Synthase-1 with Substrates and Inhibitors by Molecular Modeling and Dynamics Simulation. Journal of Physical Chemistry B, 2008, 112, 7320-7329.	1.2	22
141	Theoretical studies of nonenzymatic reaction pathways for the three reaction stages of the carboxylation of ribulose-1,5-bisphosphate. Perkin Transactions II RSC, 2001, , 23-29.	1.1	21
142	Computational Insights into the Chemical Structures and Mechanisms of the Chromogenic and Neurotoxic Effects of Aromatic γ-diketones. Journal of Physical Chemistry B, 2003, 107, 2853-2861.	1.2	21
143	Fundamental Reaction Pathway and Free Energy Profile for Hydrolysis of Intracellular Second Messenger Adenosine 3′,5′-Cyclic Monophosphate (cAMP) Catalyzed by Phosphodiesterase-4. Journal of Physical Chemistry B, 2011, 115, 12208-12219.	1.2	21
144	Reaction pathways and free energy profiles for spontaneous hydrolysis of urea and tetramethylurea: unexpected substituent effects. Organic and Biomolecular Chemistry, 2013, 11, 7595.	1.5	21

#	Article	IF	CITATIONS
145	Influence of Sugar Amine Regiochemistry on Digitoxigenin Neoglycoside Anticancer Activity. ACS Medicinal Chemistry Letters, 2015, 6, 1053-1058.	1.3	21
146	Catalytic Reaction Mechanism for Drug Metabolism in Human Carboxylesterase-1: Cocaine Hydrolysis Pathway. Molecular Pharmaceutics, 2018, 15, 3871-3880.	2.3	21
147	Maximum overlap symmetry orbitals. International Journal of Quantum Chemistry, 1991, 39, 729-746.	1.0	20
148	Maximum bond order hybrid orbitals. Theoretica Chimica Acta, 1993, 84, 511-520.	0.9	20
149	Reaction Mechanism for Cocaine Esterase-Catalyzed Hydrolyses of (+)- and (â^')-Cocaine: Unexpected Common Rate-Determining Step. Journal of Physical Chemistry B, 2011, 115, 5017-5025.	1.2	20
150	The role of human dopamine transporter in NeuroAIDS. , 2018, 183, 78-89.		20
151	Computational determination of fundamental pathway and activation barriers for acetohydroxyacid synthaseâ€catalyzed condensation reactions of αâ€keto acids. Journal of Computational Chemistry, 2010, 31, 1592-1602.	1.5	19
152	Determination of the Structure of Human Phosphodiesterase-2 in a Bound State and Its Binding with Inhibitors by Molecular Modeling, Docking, and Dynamics Simulation. Journal of Physical Chemistry B, 2009, 113, 2896-2908.	1.2	19
153	Discovery of potent and selective butyrylcholinesterase inhibitors through the use of pharmacophore-based screening. Bioorganic and Medicinal Chemistry Letters, 2019, 29, 126754.	1.0	19
154	Chromogenic and Neurotoxic Effects of an Aliphatic γ-Diketone:  Computational Insights into the Molecular Structures and Mechanism. Journal of Physical Chemistry B, 2004, 108, 6098-6104.	1.2	18
155	HIV-1 transgenic rats display an increase in [3H]dopamine uptake in the prefrontal cortex and striatum. Journal of NeuroVirology, 2016, 22, 282-292.	1.0	18
156	Binding free energies for nicotine analogs inhibiting cytochrome P450 2A6 by a combined use of molecular dynamics simulations and QM/MM-PBSA calculations. Bioorganic and Medicinal Chemistry, 2014, 22, 2149-2156.	1.4	17
157	Selective immunoproteasome inhibitors with non-peptide scaffolds identified from structure-based virtual screening. Bioorganic and Medicinal Chemistry Letters, 2014, 24, 3614-3617.	1.0	17
158	Molecular mechanism: the human dopamine transporter histidine 547 regulates basal and HIV-1 Tat protein-inhibited dopamine transport. Scientific Reports, 2016, 6, 39048.	1.6	17
159	Computational modeling of human dopamine transporter structures, mechanism and its interaction with HIV-1 transactivator of transcription. Future Medicinal Chemistry, 2016, 8, 2077-2089.	1.1	17
160	Par-4 secretion: stoichiometry of 3-arylquinoline binding to vimentin. Organic and Biomolecular Chemistry, 2016, 14, 74-84.	1.5	17
161	Development of a long-acting Fc-fused cocaine hydrolase with improved yield of protein expression. Chemico-Biological Interactions, 2019, 306, 89-95.	1.7	17
162	Theoretical calculation of the binding free energies for pyruvate dehydrogenase E1 binding with ligands. Bioorganic and Medicinal Chemistry Letters, 2007, 17, 5186-5190.	1.0	16

#	Article	IF	CITATIONS
163	An efficient implementation for determining volume polarization in self-consistent reaction field theory. Journal of Chemical Physics, 2008, 129, 194109.	1.2	16
164	Catalytic activities of a cocaine hydrolase engineered from human butyrylcholinesterase against (+)- and (â^')-cocaine. Chemico-Biological Interactions, 2013, 203, 57-62.	1.7	16
165	Kinetic characterization of a cocaine hydrolase engineered from mouse butyrylcholinesterase. Biochemical Journal, 2015, 466, 243-251.	1.7	16
166	Maximum bond order hybrid orbitals II. Correlativity with C-H and C-C spin-coupling constants. Theoretica Chimica Acta, 1993, 84, 521-533.	0.9	15
167	A three-point method for evaluations of AMBER force field parameters: an application to copper-based artificial nucleases. Theoretical Chemistry Accounts, 2009, 122, 167-178.	0.5	15
168	Plants as a source of butyrylcholinesterase variants designed for enhanced cocaine hydrolase activity. Chemico-Biological Interactions, 2013, 203, 217-220.	1.7	15
169	Catalytic mechanism of cytochrome P450 for N-methylhydroxylation of nicotine: reaction pathways and regioselectivity of the enzymatic nicotine oxidation. Dalton Transactions, 2013, 42, 3812.	1.6	15
170	Role of Histidine 547 of Human Dopamine Transporter in Molecular Interaction with HIV-1 Tat and Dopamine Uptake. Scientific Reports, 2016, 6, 27314.	1.6	15
171	Effectiveness of a Cocaine Hydrolase for Cocaine Toxicity Treatment in Male and Female Rats. AAPS Journal, 2018, 20, 3.	2.2	15
172	Semisynthetic aurones inhibit tubulin polymerization at the colchicine-binding site and repress PC-3 tumor xenografts in nude mice and myc-induced T-ALL in zebrafish. Scientific Reports, 2019, 9, 6439.	1.6	15
173	An Underlying Mechanism of Dual Wnt Inhibition and AMPK Activation: Mitochondrial Uncouplers Masquerading as Wnt Inhibitors. Journal of Medicinal Chemistry, 2019, 62, 11348-11358.	2.9	15
174	Binding Modes and Selectivity of Cannabinoid 1 (CB1) and Cannabinoid 2 (CB2) Receptor Ligands. ACS Chemical Neuroscience, 2020, 11, 3455-3463.	1.7	15
175	Reply to Ma and Wang: Reliability of various in vitro activity assays on SARS-CoV-2 main protease inhibitors. Proceedings of the National Academy of Sciences of the United States of America, 2021, 118, .	3.3	15
176	Understanding human 15-hydroxyprostaglandin dehydrogenase binding with NAD+ and PGE2 by homology modeling, docking and molecular dynamics simulation. Bioorganic and Medicinal Chemistry, 2005, 13, 4544-4551.	1.4	14
177	Dynamic structures of phosphodiesteraseâ€5 active site by combined molecular dynamics simulations and hybrid quantum mechanical/molecular mechanical calculations. Journal of Computational Chemistry, 2008, 29, 1259-1267.	1.5	14
178	Binding structures and energies of the human neonatal Fc receptor with human Fc and its mutants by molecular modeling and dynamics simulations. Molecular BioSystems, 2013, 9, 3047.	2.9	14
179	Novel Mycosin Protease MycP ₁ Inhibitors Identified by Virtual Screening and 4D Fingerprints. Journal of Chemical Information and Modeling, 2014, 54, 1166-1173.	2.5	14
180	Amino-acid mutations to extend the biological half-life of a therapeutically valuable mutant of human butyrylcholinesterase. Chemico-Biological Interactions, 2014, 214, 18-25.	1.7	14

#	Article	IF	CITATIONS
181	Allosteric modulatory effects of SRI-20041 and SRI-30827 on cocaine and HIV-1 Tat protein binding to human dopamine transporter. Scientific Reports, 2017, 7, 3694.	1.6	14
182	In vivo characterization of toxicity of norcocaethylene and norcocaine identified as the most toxic cocaine metabolites in male mice. Drug and Alcohol Dependence, 2019, 204, 107462.	1.6	14
183	Catalytic Roles of Coenzyme Pyridoxal-5′-phosphate (PLP) in PLP-Dependent Enzymes: Reaction Pathway for Methionine-γ-Lyase-Catalyzed <scp>l</scp> -Methionine Depletion. ACS Catalysis, 2020, 10, 2198-2210.	5.5	14
184	Epigenetic Regulation of Wnt Signaling by Carboxamide-Substituted Benzhydryl Amines that Function as Histone Demethylase Inhibitors. IScience, 2020, 23, 101795.	1.9	14
185	Replenishing HDL with synthetic HDL has multiple protective effects against sepsis in mice. Science Signaling, 2022, 15, eabl9322.	1.6	14
186	Reaction Pathway and Free Energy Profile for Prechemical Reaction Step of Human Butyrylcholinesterase-Catalyzed Hydrolysis of (â``)-Cocaine by Combined Targeted Molecular Dynamics and Potential of Mean Force Simulations. Journal of Physical Chemistry B, 2010, 114, 13545-13554.	1.2	13
187	Interaction of tyrosine 151 in norepinephrine transporter with the 2β group of cocaine analog RTI-113. Neuropharmacology, 2011, 61, 112-120.	2.0	13
188	Cocaine Esterase–Cocaine Binding Process and the Free Energy Profiles by Molecular Dynamics and Potential of Mean Force Simulations. Journal of Physical Chemistry B, 2012, 116, 3361-3368.	1.2	13
189	Unexpected Reaction Pathway for butyrylcholinesterase-catalyzed inactivation of "hunger hormone― ghrelin. Scientific Reports, 2016, 6, 22322.	1.6	13
190	Selective inhibitors of human mPGES-1 from structure-based computational screening. Bioorganic and Medicinal Chemistry Letters, 2017, 27, 3739-3743.	1.0	13
191	Development of Fc-Fused Cocaine Hydrolase for Cocaine Addiction Treatment: Catalytic and Pharmacokinetic Properties. AAPS Journal, 2018, 20, 53.	2.2	13
192	DREAM-in-CDM Approach and Identification of a New Generation of Anti-inflammatory Drugs Targeting mPGES-1. Scientific Reports, 2020, 10, 10187.	1.6	13
193	Generalized relationship for calculation of nuclear spin—spin coupling constants between directly bonded carbon and hydrogen atoms. Magnetic Resonance in Chemistry, 1994, 32, 465-467.	1.1	12
194	Human Butyrylcholinesterase–Cocaine Binding Pathway and Free Energy Profiles by Molecular Dynamics and Potential of Mean Force Simulations. Journal of Physical Chemistry B, 2011, 115, 11254-11260.	1.2	12
195	New inhibitor of 3-phosphoinositide dependent protein kinase-1 identified from virtual screening. Bioorganic and Medicinal Chemistry Letters, 2012, 22, 1629-1632.	1.0	12
196	Application of the 4D Fingerprint Method with a Robust Scoring Function for Scaffold-Hopping and Drug Repurposing Strategies. Journal of Chemical Information and Modeling, 2014, 54, 2834-2845.	2.5	12
197	Structure-based virtual screening leading to discovery of highly selective butyrylcholinesterase inhibitors with solanaceous alkaloid scaffolds. Chemico-Biological Interactions, 2019, 308, 372-376.	1.7	12
198	Clinical potential of a rationally engineered enzyme for treatment of cocaine dependence: Long-lasting blocking of the psychostimulant, discriminative stimulus, and reinforcing effects of cocaine. Neuropharmacology, 2020, 176, 108251.	2.0	12

#	Article	IF	CITATIONS
199	Structure-Based Design and Discovery of a Long-Acting Cocaine Hydrolase Mutant with Improved Binding Affinity to Neonatal Fc Receptor for Treatment of Cocaine Abuse. AAPS Journal, 2020, 22, 62.	2.2	12
200	Catalytic activities of cocaine hydrolases against the most toxic cocaine metabolite norcocaethylene. Organic and Biomolecular Chemistry, 2020, 18, 1968-1977.	1.5	12
201	Synthesis, Molecular Pharmacology, and Structure–Activity Relationships of 3-(Indanoyl)indoles as Selective Cannabinoid Type 2 Receptor Antagonists. Journal of Medicinal Chemistry, 2021, 64, 6381-6396.	2.9	12
202	Novel pharmacological approaches to treatment of drug overdose and addiction. Expert Review of Clinical Pharmacology, 2009, 2, 1-4.	1.3	11
203	Mechanistic insights into the substrate recognition of PPO: toward the rational design of effective inhibitors. Future Medicinal Chemistry, 2014, 6, 597-599.	1.1	11
204	Molecular modeling and redesign of alginate lyase from <i>Pseudomonas aeruginosa</i> for accelerating CRPA biofilm degradation. Proteins: Structure, Function and Bioinformatics, 2016, 84, 1875-1887.	1.5	11
205	Design, synthesis, and discovery of 5-((1,3-diphenyl-1 H -pyrazol-4-yl)methylene)pyrimidine-2,4,6(1 H ,3 H ,5) Tj ETG Letters, 2018, 28, 858-862.	Qq1 1 0.7 1.0	784314 rg <mark>8</mark> T 11
206	Key NAD+-binding residues in human 15-hydroxyprostaglandin dehydrogenase. Archives of Biochemistry and Biophysics, 2005, 433, 447-453.	1.4	10
207	Halogenated diarylacetylenes repress c-myc expression in cancer cells. Bioorganic and Medicinal Chemistry Letters, 2014, 24, 3638-3640.	1.0	10
208	Kinetic characterization of cholinesterases and a therapeutically valuable cocaine hydrolase for their catalytic activities against heroin and its metabolite 6-monoacetylmorphine. Chemico-Biological Interactions, 2018, 293, 107-114.	1.7	10
209	Effects of Cebranopadol on Cocaine-induced Hyperactivity and Cocaine Pharmacokinetics in Rats. Scientific Reports, 2020, 10, 9254.	1.6	10
210	The H•/H [–] Redox Couple and Absolute Hydration Energy of H [–] . Journal of Physical Chemistry A, 2020, 124, 6084-6095.	1.1	10
211	Maximum overlap method and the bond strength. International Journal of Quantum Chemistry, 1987, 32, 1-11.	1.0	9
212	The molecular basis of talin2's high affinity toward β1-integrin. Scientific Reports, 2017, 7, 41989.	1.6	9
213	Reengineering of Albumin-Fused Cocaine Hydrolase CocH1 (TV-1380) to Prolong Its Biological Half-Life. AAPS Journal, 2020, 22, 5.	2.2	9
214	Development of a Highly Efficient Long-Acting Cocaine Hydrolase Entity to Accelerate Cocaine Metabolism. Bioconjugate Chemistry, 2022, 33, 1340-1349.	1.8	9
215	QSAR study on maximal inhibition (Imax) of quaternary ammonium antagonists for S-(â^')-nicotine-evoked dopamine release from dopaminergic nerve terminals in rat striatum. Bioorganic and Medicinal Chemistry, 2009, 17, 4477-4485.	1.4	8
216	Characterization of the Structures of Phosphodiesterase 10 Binding with Adenosine 3′,5′-Monophosphate and Guanosine 3′,5′-Monophosphate by Hybrid Quantum Mechanical/Molecular Mechanical Calculations. Journal of Physical Chemistry B, 2010, 114, 7022-7028.	1.2	8

#	Article	IF	CITATIONS
217	Computational Modeling of Solvent Effects on Protein-Ligand Interactions Using Fully Polarizable Continuum Model and Rational Drug Design. Communications in Computational Physics, 2013, 13, 31-60.	0.7	8
218	Blocking drug activation as a therapeutic strategy to attenuate acute toxicity and physiological effects of heroin. Scientific Reports, 2018, 8, 16762.	1.6	8
219	Mutational effects of human dopamine transporter at tyrosine88, lysine92, and histidine547 on basal and HIV-1 Tat-inhibited dopamine transport. Scientific Reports, 2019, 9, 3843.	1.6	8
220	Cocaine hydrolase blocks cocaineâ€induced dopamine transporter trafficking to the plasma membrane. Addiction Biology, 2022, 27, e13089.	1.4	8
221	Pauling's criterion of bond strength and the relative bond lengths in molecule MLk. International Journal of Quantum Chemistry, 1991, 40, 675-683.	1.0	7
222	Molecular equilibrium geometries and vibrational frequencies by maximum overlap symmetry molecular orbital method. International Journal of Quantum Chemistry, 1992, 41, 773-783.	1.0	7
223	Computational neural network analysis of the affinity of N-n-alkylnicotinium salts for the α4β2* nicotinic acetylcholine receptor. Journal of Enzyme Inhibition and Medicinal Chemistry, 2009, 24, 157-168.	2.5	7
224	Computational gibberellinâ€binding channel discovery unraveling the unexpected perception mechanism of hormone signal by gibberellin receptor. Journal of Computational Chemistry, 2013, 34, 2055-2064.	1.5	7
225	A novel and efficient ligand-based virtual screening approach using the HWZ scoring function and an enhanced shape-density model. Journal of Biomolecular Structure and Dynamics, 2013, 31, 1236-1250.	2.0	7
226	A model of glycosylated human butyrylcholinesterase. Molecular BioSystems, 2014, 10, 348-354.	2.9	7
227	Reaction pathway and free energy barrier for urea elimination in aqueous solution. Chemical Physics Letters, 2015, 625, 143-146.	1.2	7
228	Effects of a cocaine hydrolase engineered from human butyrylcholinesterase on metabolic profile of cocaine in rats. Chemico-Biological Interactions, 2016, 259, 104-109.	1.7	7
229	A Practical System for High-Throughput Screening of Mutants of Bacillus fastidiosus Uricase. Applied Biochemistry and Biotechnology, 2017, 181, 667-681.	1.4	7
230	Generalized Methodology for the Quick Prediction of Variant SARS-CoV-2 Spike Protein Binding Affinities with Human Angiotensin-Converting Enzyme II. Journal of Physical Chemistry B, 2022, 126, 2353-2360.	1.2	7
231	Development of pharmacotherapies for abdominal aortic aneurysms. Biomedicine and Pharmacotherapy, 2022, 153, 113340.	2.5	7
232	Theoretical studies of reaction pathways and energy barriers for alkaline hydrolysis of phosphotriesterase substrates paraoxon and related toxic phosphofluoridate nerve agents. Perkin Transactions II RSC, 2001, , 2355-2363.	1.1	6
233	Unveiling the Unfolding Pathway of F5F8D Disorder-Associated D81H/V100D Mutant of MCFD2 <i>via</i> Multiple Molecular Dynamics Simulations. Journal of Biomolecular Structure and Dynamics, 2012, 29, 699-714.	2.0	6
234	Facile Alkaline Lysis of Escherichia coli Cells in High-Throughput Mode for Screening Enzyme Mutants: Arylsulfatase as an Example. Applied Biochemistry and Biotechnology, 2016, 179, 545-557.	1.4	6

#	Article	IF	CITATIONS
235	In Silico Observation of the Conformational Opening of the Glutathione-Binding Site of Microsomal Prostaglandin E2 Synthase-1. Journal of Chemical Information and Modeling, 2019, 59, 3839-3845.	2.5	6
236	Development of a novel prostate apoptosis response-4 (Par-4) protein entity with an extended duration of action for therapeutic treatment of cancer. Protein Engineering, Design and Selection, 2019, 32, 159-166.	1.0	6
237	Cebranopadol reduces cocaine self-administration in male rats: Dose, treatment and safety consideration. Neuropharmacology, 2020, 172, 108128.	2.0	6
238	Recovery of dopaminergic system after cocaine exposure and impact of a longâ€acting cocaine hydrolase. Addiction Biology, 2022, 27, .	1.4	6
239	Potential anti-obesity effects of a long-acting cocaine hydrolase. Chemico-Biological Interactions, 2016, 259, 99-103.	1.7	5
240	A Numerical Approach for Kinetic Analysis of the Nonexponential Thermoinactivation Process of Uricase. Protein Journal, 2016, 35, 318-329.	0.7	5
241	Plant expression of cocaine hydrolase-Fc fusion protein for treatment of cocaine abuse. BMC Biotechnology, 2016, 16, 72.	1.7	5
242	Cocaine Hydrolases Designed from Butyrylcholinesterase. , 2016, , 187-225.		5
243	MBOHO calculations of C?H stretching frequencies in hydrocarbons and heterosubstituted hydrocarbons. International Journal of Quantum Chemistry, 1994, 52, 109-116.	1.0	4
244	MBOHO calculations of carbon-nitrogen nuclear spin-spin coupling constants. Magnetic Resonance in Chemistry, 1995, 33, 249-251.	1.1	4
245	First-Principles Determination of Molecular Conformations of Cyclic Adenosine 3′,5′-Monophosphate in Gas Phase and Aqueous Solution. Journal of Physical Chemistry B, 2008, 112, 16851-16859.	1.2	4
246	Microscopic binding of butyrylcholinesterase with quinazolinimine derivatives and the structure–activity correlation. Theoretical Chemistry Accounts, 2011, 130, 69-82.	0.5	4
247	Microscopic modes and free energies for topoisomerase I-DNA covalent complex binding with non-camptothecin inhibitors by molecular docking and dynamics simulations. Theoretical Chemistry Accounts, 2013, 132, 1.	0.5	4
248	Mccrearamycins A–D, Geldanamycinâ€Đerived Cyclopentenone Macrolactams from an Eastern Kentucky Abandoned Coal Mine Microbe. Angewandte Chemie, 2017, 129, 3040-3044.	1.6	4
249	Dimerization of human butyrylcholinesterase expressed in bacterium for development of a thermally stable bioscavenger of organophosphorus compounds. Chemico-Biological Interactions, 2019, 310, 108756.	1.7	4
250	OleD Loki as a Catalyst for Hydroxamate Glycosylation. ChemBioChem, 2020, 21, 952-957.	1.3	4
251	7-Azaindolequinuclidinones (7-AIQD): A novel class of cannabinoid 1 (CB1) and cannabinoid 2 (CB2) receptor ligands. Bioorganic and Medicinal Chemistry Letters, 2020, 30, 127501.	1.0	4
252	Pictet–Spengler condensations using 4-(2-aminoethyl)coumarins. New Journal of Chemistry, 2020, 44, 13415-13429.	1.4	4

#	Article	IF	CITATIONS
253	A plant-derived cocaine hydrolase prevents cocaine overdose lethality and attenuates cocaine-induced drug seeking behavior. Progress in Neuro-Psychopharmacology and Biological Psychiatry, 2020, 102, 109961.	2.5	4
254	Binding Mode of Human Norepinephrine Transporter Interacting with HIV-1 Tat. ACS Chemical Neuroscience, 2021, 12, 1519-1527.	1.7	4
255	Indole-Containing Amidinohydrazones as Nonpeptide, Dual RXFP3/4 Agonists: Synthesis, Structure–Activity Relationship, and Molecular Modeling Studies. Journal of Medicinal Chemistry, 2021, 64, 17866-17886.	2.9	4
256	Fast Prediction of Binding Affinities of SARS-CoV-2 Spike Protein and Its Mutants with Antibodies through Intermolecular Interaction Modeling-Based Machine Learning. Journal of Physical Chemistry B, 2022, 126, 5194-5206.	1.2	4
257	First-principles determination of molecular conformations of indolizidine (â^')-235B′ in solution. Theoretical Chemistry Accounts, 2009, 124, 269-278.	0.5	3
258	Structural Assignment of 6-Oxy Purine Derivatives through Computational Modeling, Synthesis, X-ray Diffraction, and Spectroscopic Analysis. Journal of Physical Chemistry B, 2010, 114, 6968-6972.	1.2	3
259	Sulfhydryl-specific PEGylation of phosphotriesterase cysteine mutants for organophosphate detoxification. Protein Engineering, Design and Selection, 2015, 28, 501-506.	1.0	3
260	High-throughput estimation of specific activities of enzyme/mutants in cell lysates through immunoturbidimetric assay of proteins. Analytical Biochemistry, 2017, 534, 91-98.	1.1	3
261	Actions of Butyrylcholinesterase Against Cocaine. , 2017, , 663-672.		3
262	Phenylethynyl-substituted heterocycles inhibit cyclin D1 and induce the expression of cyclin-dependent kinase inhibitor p21Wif1/Cip1 in colorectal cancer cells. MedChemComm, 2018, 9, 87-99.	3.5	3
263	Correlations between the 1H NMR chemical shieldings and the pKa values of organic acids and amines. Journal of Molecular Modeling, 2018, 24, 146.	0.8	3
264	Correlation between the pKa and nuclear shielding of α-hydrogen of ketones. Journal of Molecular Modeling, 2019, 25, 354.	0.8	3
265	A THEORETICAL STUDY ON CORRELATION BETWEEN THE STRUCTURES AND 31P NMR CHEMICAL SHIFTS OF DICOORDINATED PHOSPHENIUM CATIONS. Phosphorus, Sulfur and Silicon and the Related Elements, 1997, 126, 89-99.	0.8	2
266	MAXIMUM BOND ORDER HYBRID ORBITAL CALCULATIONS OF' THE SËO STRETCHING FREQUENCIES FOR SULPHURYL AND THIONYL COMPOUNDS. Phosphorus, Sulfur and Silicon and the Related Elements, 1999, 149, 65-73.	0.8	2
267	GENERALIZED CORRELATION OF P[dbnd]O AND P[dbnd]S BOND STRETCHING VIBRATIONAL FREQUENCIES WITH ELECTRONIC STRUCTURE IN ORGANOPHOSPHORUS COMPOUNDS. Phosphorus, Sulfur and Silicon and the Related Elements, 2000, 157, 67-85.	0.8	2
268	Modeling Reaction Mechanism of Cocaine Hydrolysis and Rational Drug Design for Therapeutic Treatment of Cocaine Abuse. , 0, , 107-159.		2
269	Protein flexibility and conformational states of <i>Leishmania</i> antigen eIF-4A: identification of a novel plausible protein adjuvant using comparative genomics and molecular modeling. Journal of Biomolecular Structure and Dynamics, 2013, 31, 841-853.	2.0	2
270	Reaction pathway for cocaine hydrolase-catalyzed hydrolysis of (+)-cocaine. Theoretical Chemistry Accounts, 2016, 135, 1.	0.5	2

#	Article	IF	CITATIONS
271	Polyclonal Antibodies in Microplates to Predict the Maximum Adsorption Activities of Enzyme/Mutants from Cell Lysates. Protein Journal, 2017, 36, 212-219.	0.7	2
272	Design, synthesis, and biological activity of 5′-phenyl-1,2,5,6-tetrahydro-3,3′-bipyridine analogues as potential antagonists of nicotinic acetylcholine receptors. Bioorganic and Medicinal Chemistry Letters, 2017, 27, 4350-4353.	1.0	2
273	Flipped Phenyl Ring Orientations of Dopamine Binding with Human and Drosophila Dopamine Transporters: Remarkable Role of Three Nonconserved Residues. ACS Chemical Neuroscience, 2018, 9, 1426-1431.	1.7	2
274	Oligomerization and Catalytic Parameters of Human UDP-Glucuronosyltransferase 1A10: Expression and Characterization of the Recombinant Protein. Drug Metabolism and Disposition, 2018, 46, 1446-1452.	1.7	2
275	PEGylation but Not Fc-Fusion Improves in Vivo Residence Time of a Thermostable Mutant of Bacterial Cocaine Esterase. Bioconjugate Chemistry, 2019, 30, 3021-3027.	1.8	2
276	Systematic Structure-Based Virtual Screening Approach to Antibody Selection and Design of a Humanized Antibody against Multiple Addictive Opioids without Affecting Treatment Agents Naloxone and Naltrexone. ACS Chemical Neuroscience, 2021, 12, 184-194.	1.7	2
277	MBOHO calculations of phosphorus-carbon nuclear spin-spin coupling constants. Theoretica Chimica Acta, 1995, 92, 61-65.	0.9	1
278	Structural features and binding free energies for non-covalent inhibitors interacting with immunoproteasome by molecular modeling and dynamics simulations. Theoretical Chemistry Accounts, 2012, 131, 1.	0.5	1
279	Striking Effects of Storage Buffers on Apparent Half-Lives of the Activity of Pseudomonas aeruginosa Arylsulfatase. Protein Journal, 2016, 35, 283-290.	0.7	1
280	Free energy profiles of cocaine esterase-cocaine binding process by molecular dynamics and potential of mean force simulations. Chemico-Biological Interactions, 2016, 259, 142-147.	1.7	1
281	Extracorporeal delivery of a therapeutic enzyme. Scientific Reports, 2016, 6, 30888.	1.6	1
282	Regioselective synthesis of 2- and 4-diarylpyridine ethers and their inhibitory activities against phosphodiesterase 4B. Journal of Molecular Structure, 2019, 1196, 455-461.	1.8	1
283	Efficient Cocaine Degradation by Cocaine Esterase-Loaded Red Blood Cells. Frontiers in Physiology, 2020, 11, 573492.	1.3	1
284	The crystal structure of <scp>AbsH3</scp> : A putative flavin adenine dinucleotideâ€dependent reductase in the abyssomicin biosynthesis pathway. Proteins: Structure, Function and Bioinformatics, 2021, 89, 132-137.	1.5	1
285	Clinical data mining reveals analgesic effects of lapatinib in cancer patients. Scientific Reports, 2021, 11, 3528.	1.6	1
286	Reply to Behnam and Klein: Potential role of the His-tag in C-terminal His-tagged SARS-CoV-2 main protease. Proceedings of the National Academy of Sciences of the United States of America, 2021, 118, .	3.3	1
287	Enzyme-Based Cocaine Pharmacotherapies: Current Status and Projections for the Future. , 2016, , 145-166.		1
288	Reply to Curry and Coombs: Benzoic acid is formed predominantly from the benzoyl ester hydrolysis in the presence of cocaine hydrolase. Proceedings of the National Academy of Sciences of the United States of America, 2016, 113, E2102-E2103.	3.3	0

#	Article	IF	CITATIONS
289	Data for high-throughput estimation of specific activities of enzyme/mutants in cell lysates through immunoturbidimetric assay of proteins. Data in Brief, 2017, 14, 220-245.	0.5	0